ELSEVIER

Sensors and Actuators A 62 (1997) 599-611

SENSORS AND ACTUATORS A PHYSICAL

Characterization of a planar microcoil for implantable microsystems

C.R. Neagu *, H.V. Jansen, A. Smith, J.G.E. Gardeniers, M.C. Elwenspoek

MESA Research Institute, University of Twente, PO Box 217, 7500 AE Enschede, Netherlands

Abstract

This paper discusses the modelling, design and characterization of planar microcoils to be used in telemetry systems that supply energy to miniaturized implants. Parasitic electrical effects that may become important at a.c. frequencies of several megahertz are evaluated. The fabrication process and electrical characterization of planar receiver microcoils will be described, and it will be shown that a power of a few milliwatts is feasible. © 1997 Elsevier Science S.A.

Keywords: Implantable microsystems; Microcoils

1. Introduction

Over the last few years, interest in and use of implants in the human body has increased. Permanent implants can be used for continuous monitoring of certain medical parameters (e.g., insulin level, intraocular pressure) or for actuation of specific nerves [1,2]. As the implants get smaller, much attention is directed towards downscaling of the electronics, data-transmission circuitry and power supply. Considering the latter, the use of a battery is not always feasible or desirable because of size and lifetime limitations [3], while in general wire connections cannot be placed for long periods of time. An alternative is the transmission of energy by inductive coupling of a pair of coils: a transmitter coil and a receiver coil implanted in the human body as shown in Fig. 1. The receiver coil for this type of application has two important requirements: a very small size and a high efficiency.

The small size of the receiver coil might lead to the need for a dense time-varying magnetic field through this coil, in order to transfer a sufficient amount of energy. However, such a field induces eddy currents in a conductive material, such as human tissue, resulting in resistive heating or actuation of nerves. It has been reported that this heating can cause damage to human tissue [4]. So, in general dense magnetic fields are not desirable. In order to be able to transfer sufficient energy at a less dense field, the design of the receiver coil should be optimized.

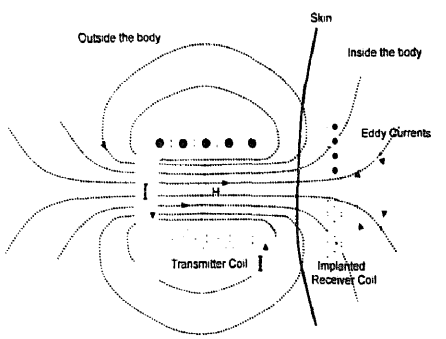

Fig. 1. Cross section of a transmitter–receiver set-up showing magnetic field lines.

In this paper we shall focus on different configurations of planar receiver coils made with the use of so-called micromachining technologies such as thin-film deposition and electroplating. With this technology small coils are relatively easy to fabricate reproducibly. Insight has been gained into the importance of parasitic effects, which start dominating at frequencies of several megahertz. First, a model of the electrical characteristics of planar coils will be discussed, followed by a discussion of design configurations and fabrication procedures. The parameters of fabricated coils will be evaluated by electrical measurements, and first results of the energy transfer from a conventional coil to the planar coil will be presented. However, before starting we shall have a closer look at the energy transfer needed to feed the receiver electronics, i.e., the telemetry.

* Corresponding author. Tel.: +31 53 489 2805. Fax: +31 53 489 3343. E-mail: c.neagu@el.utwente.nl

PII S0924-4247(97)01601-4

2. Telemetry

Currently, the transport of energy by way of inductive coupling between a set of coils is found in almost any electronic apparatus. The energy transfer is accomplished by using two coils: a transmitter coil that supplies the energy in the form of a magnetic field and a receiver coil to collect as much as possible energy from this field. Generally, when the coils are allowed to be in close contact, a transformer is used. In the transformer, the magnetic field is directed from the transmitter coil into the receiver coil by way of a magnetically conducting medium like iron. At a greater distance, it is no longer possible to use iron to concentrate the magnetic field. Therefore, the coils have to be aligned in order to couple enough energy.

When the frequency of the field, generated by the transmitter coil, is higher than a few kilohertz, the transmission of electromagnetic energy by electromagnetic waves (EM-waves) becomes efficient. EM-waves have their application in a broad frequency spectrum from several kilohertz up to many gigahertz. For example, in a microwave oven working at a few gigahertz, energy is transferred into water molecules to heat up a meal. The advantage of EM-waves is that they can be directed with the use of special antennae. Due to this characteristic, it is possible to direct energy over quite a large distance without any problem. Moreover, it is possible to modulate the EM-wave, i.e., the carrier signal, with data in order to transmit information wirelessly. This is the field of telecommunications, without doubt one of the most important pillars of modern human society. It is found in applications such as radio and television, but it is also used to control an object at a distance, as in the case of a remote controller to zap your television set or a small battery-powered transmitter to steer a model aeroplane flying through the sky.

Frequently, it is necessary to transport information from a sensing or measuring unit to a remote controller and back again: this is the field of telemetry. Data are now going in both directions. The remote system is not only receiving its control signals but also transmits its measured data. For this reason, such systems are generally called transceivers, the joining of the words transmitter and receiver. Exciting examples of this field are the Voyager spacecraft which explore the universe.

In some special cases, the remote transceiver has not the possibility to supply the energy to feed its own electronics. These electronics are necessary to prepare the data to be sent to the transmitter or host coil. In such cases, the host coil is not only used to transmit the control signals but it is also used to transport the energy for the electronics of the remote transceiver. In such cases, after stripping an EM-wave from its control signals, the carrier signal is rectified in order to supply the electronics with this energy. It is obvious that this type of communication is one of the most challenging technologies in use in telemetry nowadays, because the carrier signal not only carries the energy but the data too. Nevertheless, in the case of human implants, this technology seems to be one of the few possibilities to control functions in a "human friendly" way.

Therefore, in the remaining part of this section we shall concentrate on aspects with respect to the energy received by a remote receiver coil and how this energy is directed to its electronics. Although the system also has to communicate by way of control signals and sensed data, this subject is not discussed here. We do not mean to imply that this subject is unimportant, but mainly that it is not of our concern in this paper.

In order to find the governing equations that describe the transfer of energy and efficiency in a receiving coil, we shall start with some aspects dealing with energy transfer and efficiency. Fig. 2 is a schematic drawing of the transceiver part of a telemetric system. It consists of a host system which transmits an energy E_{trans} and a remote unit which receives only a part of this energy E_{rec} due to the distance between both units and the divergence of the EM-field. The received energy, in turn, is partly dissipated as Joule heat E_{dis} in the resistance of the receiver coil and the energy left is stored as EM-energy E_{EM} in the self-inductance L and capacitance C of this coil, i.e., the LC-circuit. Finally, a part of the EM-energy stored can be used to supply the electronics with the requested energy E_{elec}, that is, it will be dissipated in a load resistance. Now, when we look at the receiving remote unit it is possible to define a quality-factor Q_{rec} as (Fig. 2)

$$Q_{rec} = \frac{E_{EM}}{E_{dis}} \tag{1a}$$

So, the Q-factor is a measure of the efficiency of the receiver coil. The higher the Q-factor, the better the performance with respect to the energy transfer will be. Note that, for maximum energy transfer from the stored EM-energy to the load resistance, we have to optimize the load resistance. This can be achieved by matching the load resistance to the characteristic impedance of the LC-circuit, but this subject will be treated later.

Another familiar equation to describe the efficiency of the receiver coil is by looking at the plot of the impedance or output voltage of the coil as a function of the frequency. In this case the operation quality-factor, Q_o, turns out to be (Fig. 2)

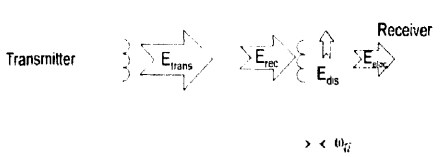

Fig. 2. Schematic drawing of the energies involved in the transceiver part of a telemetric system. The receiver coil has to have a high efficiency, i.e., sharp resonance peak, while the transmitter coil does not (see text); ω_o is the working or operating resonance frequency and ω_{-3} denotes the width of the resonance curve at half maximum of the output voltage.

$$Q_s = \frac{\omega_0}{\omega_{\sqrt{2}}} \tag{1b}$$

In this formulation ω_0 is the working or operating resonance frequency and $\omega_{\sqrt{2}}$ denotes the width of the resonance curve at $1/2\sqrt{2} \sim 0.707$ times the maximum of the output voltage, as shown in Fig. 2. Note that when the output function is the transferred power, this point is taken at half maximum because $P = U^2/R$. So, a sharp peak in the resonance curve is indicative of a high efficiency. If both the transmitter and receiver coil have a sharp resonance peak, it would be difficult to tune both circuits at the same frequency. However, the transmitter coil is not restricted to have a high efficiency because it does not have to be implanted and therefore the supply of energy for this coil is not restricted. Therefore, the Q-factor or efficiency of the transmitter coil is chosen to be low, to allow for easy tuning of both coils.

So, we have already found two ways to determine the efficiency of the remote receiving unit. Yet, there is still another practical definition found in the literature which uses the intrinsic characteristics of the receiving coil, i.e., the self-inductance L, parasitic capacitance C_{par} and series resistance R_S. When the coil with these three intrinsic components is left on its own (i.e., no extra circuitry such as a load is connected to the coil) and the coil is activated by an external alternating field, the circuit starts to oscillate at a specific frequency, the intrinsic resonance frequency ω_i [rad s^{-1}]:

$$\omega_i = \sqrt{\frac{1}{LC_{par}} - \frac{R_S^2}{L^2}} \sim \sqrt{\frac{1}{LC_{par}}} \tag{2a}$$

The approximation on the right-hand side of Eq. (2a) is only allowed under the condition that $R_S \ll \omega_i L$. Generally in electronics, the receiving coil is not left on its own to determine the resonance frequency. Instead, an extra tuning capacitor, C_{tune}, is placed in parallel with the coil to be able to tune for the desired operating resonance frequency, ω_0. In such cases, the resonance frequency can be found by adjusting Eq. (2a) for this capacitance:

$$\omega_0 \sim \sqrt{\frac{1}{L(C_{par} + C_{tune})}} \tag{2b}$$

So, in many practical situations, the real resonance frequency is lower than the intrinsic resonance frequency. Now we go back to Eq. (1a). In this equation, the energy for the electronics is supplied by the energy stored in the magnetic field of the self-inductance of the coil and the dissipated energy is due to the series resistance. When there is no load connected to the LC-circuit, the intrinsic Q-factor Q_i (which is the ratio between the energy that can be used for the load and the energy dissipated in the coil) becomes

$$Q_i = \frac{E_L}{E_{R_S}} = \frac{\omega_i L}{R_S} = \sqrt{\frac{L}{R^2 C_{par}} - 1} \sim \frac{1}{R_S}\sqrt{\frac{L}{C_{par}}} \tag{1c}$$

The intrinsic characteristics of the coil mainly depend on geometrical factors, so, with the help of this formulation we are able to calculate the efficiency of the system beforehand and not, as in case of the first two definitions, only afterwards. This gives us the possibility to optimize the efficiency of the remote receiver coil with respect to the geometry, if and only if the intrinsic equations are known.

There is still one important issue about efficiency left: what happens to the efficiency when a load resistance and/or tuning capacitor are connected to the receiver coil in Fig. 2? In this drawing, the equivalent of the receiver coil is given as an ideal self-inductance L in series with a series resistance R_S to account for Ohmic losses. Both components are placed in parallel with a parasitic capacitance C caused by voltage differences between closely spaced conducting surfaces. The load is connected in parallel with the parasitic capacitance. There are at least two ways to look at this circuit. One is to replace the receiver coil by three individual components: a self-inductance, series resistance and a parasitic capacitance. The second method treats the coil as a distributed system. In the following, it will be shown that there is quite a remarkable difference between both approaches with respect to optimizing the load resistance.

In the *non-distributed* approach, the self-inductance with its series resistance can be replaced by an equivalent paralliel circuit of a new self-inductance L' with resistance R'. The behaviour of this purely parallel circuit is identical to that of the original one when the following conditions are fulfilled:

$$L' = L\left[1 + \left(\frac{R_S}{\omega L}\right)^2\right] \quad \text{and} \quad R' = \frac{L}{R_S C} \tag{3a}$$

resulting in Eqs. (1c) and (2a). With the help of this parallel equivalent circuit it is easy to obtain the state of maximum power transfer of the LC-circuit into the load:

$$R_{load} = R' = \frac{L}{R_S C} \tag{3b}$$

When a load capacitance is connected to the output terminals of the receiver coil, the resonance frequency will decrease in the same way as found in Eq. (2b).

In the *distributed* approach, we look at the coil as a transmission line. A transmission line, such as a coaxial cable, can be represented by N distributed circuits consisting of a self-inductance in series with a resistance, both placed in parallel with a capacitance. For such a distributed system, the characteristic impedance Z_0 is found with the help of the so-called telegraph equations. In case of maximum power transfer the load should match Z_0:

$$R_{load} = Z_0 = \sqrt{\frac{R_S + j\omega L}{G_p + j\omega C}} \sim \sqrt{\frac{L}{C}} \tag{3c}$$

The approximation at the right-hand side of this equation is only allowed when $R_S \ll j\omega L$ and $G_p = 1/R_p \ll j\omega C$, which is quite often the case. Clearly, Eqs. (3b) and (3c) are not the same. Which formulation to use depends on the resonating system we are looking at and whether it is distributed or not.

3. Theory of a planar coil

In order to have a good receiver coil, in this section a theoretical model of the intrinsic characteristics of a planar microcoil, as shown in Fig. 3, will be discussed. This will give a better understanding of the influence of parasitic effects and gives us the possibility to optimize the coil's design with respect to energy transfer. We shall concentrate on such a planar coil, because this type of coil is ideal to be manufactured in a small size by means of micromachining techniques. If the coil has to be implanted in the human body, the small size is a prerequisite. The simplified equivalent electrical circuit of the transceiver system is shown in Fig. 4. It consists of two, almost identical, inductively coupled circuits: the transmitter and receiver units. Both units have an *LC*-circuit, which can be driven in resonance. Due to imperfections in the conductors and insulators, the coils do have a finite (small) series resistance, R_S, and the capacitances a (big) parallel resistance R_p, respectively. These resistors dissipate energy (Joule heat) and, therefore, they will lower the efficiency of the resonance circuits as expressed by Eq. (1a). So, the dissipated energy is directly influenced by the series resistance, which depends on geometrical factors. The received energy mainly depends on the self-inductance of the coil, which also depends on the dimensions of the coil. Therefore, a theoretical analysis is necessary to be able to find criteria to obtain an optimum performance of the receiver coil.

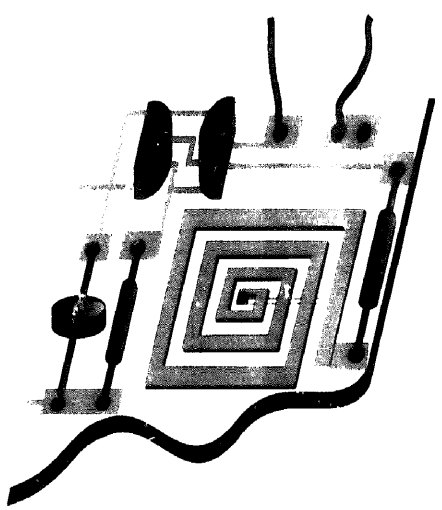

Fig. 3. Simplified representation of a planar receiver coil with some electric components.

Different complex classical formulae and approximations for coil parameters are in use, depending on the geometry of the coil and the desired degree of accuracy [5–15,18]. In this study, we shall only consider copper coils, deposited on a silicon substrate covered with an insulating silicon oxide film. The electrical behaviour of such a planar microcoil depends on the inductance L_r, the conductor series resistance R_S, the parasitic capacitance, C_r, and the insulator (substrate) resistance R_p. These parameters will now be treated one by one.

3.1. Self-inductance

The self-inductance of a coil, L, is defined as the magnetic flux linkage per unit current in the coil itself. Alternatively, it is defined as twice the energy stored in the magnetic field divided by the square of the current through the coil. In 1943, Terman arrived at some expressions for the low-frequency, i.e., no skin-effect, self-inductance of differently shaped coils [18]. We shall start with expressions for a single turn or loop and then increase the number of turns to increase the self-inductance drastically. The self-inductance of a rectangle of sides s_1 [m] and s_2 [m] and diagonal g [m] of wire of diameter d [m] is ([18], Eq. (33))

$$L_r\,[\mathrm{H}] = \frac{\mu}{\pi}\left[(s_1+s_2)\ln\frac{4s_1s_2}{d} - s_1\ln(s_1+g) - s_2\ln(s_2+g) + d + 2g - 2s_1 - 2s_2\right] \tag{4a}$$

where $\mu = 4\pi\times 10^{-7}$ [H m^{-1}] is the relative permeability of air. In the case of a square, $s_1 = s_2 = D$ and $g = s\sqrt{2}$, this expression turns into ([18], Eq. (32))

$$L_r\,[\mathrm{H}] = \frac{2\mu D}{\pi}\left[\ln\frac{2D}{d} + \frac{d}{2D} - 0.774\right] \tag{4b}$$

Generally, in micromachining, the shape of the wire of a planar microcoil is not round but rectangular of thickness b and height h as shown in Fig. 5. Then, Eq. (4b) becomes

$$L_r\,[\mathrm{H}] = \frac{2\mu D}{\pi}\left[\ln\frac{4D}{b+h} + 0.894\frac{b+h}{4D} - 0.660\right] \tag{4c}$$

When we take $D = 4.5$ mm and $h = b = 10$ μm, the self-inductance is approximately 20 nH. Making $h = b = 1$ μm, the self-

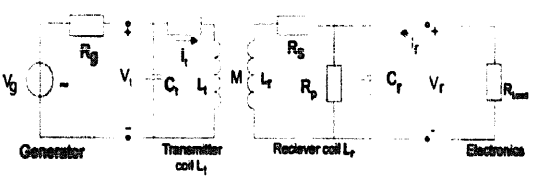

Fig. 4. Simplified equivalent electrical circuit of the transceiver system: the transmitter system coupled with the non-ideal receiver coil.

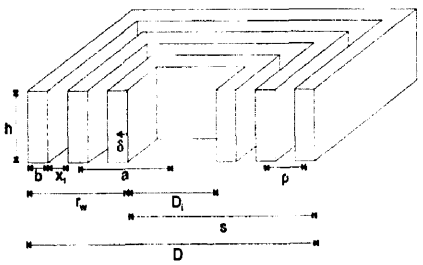

Fig. 5. Schematic cross section of a square, planar microcoil showing the geometrical parameters and the relation between them. D = diameter of the coil, r_w = winding depth, b = width of wire, h = height of wire, a = mean radius of the coil, D_i = internal diameter, δ = current penetration depth, x_1 = distance between two adjacent turns, p = pitch, i.e., distance between axes of two adjacent turns, $\alpha = D_i/D$, $p = x_1 + b$, $r_w = (D_e - D)/2 = D(1-\alpha)/2$, $a = (D_i + D)/4 = D(1+\alpha)/4$, $s = D_i + r_w = D(1+\alpha)/2$, $N = R_w/p = D(1-\alpha)/2p$.

inductance only slightly increases to 30 nH. So, the influence of the cross section of the wire on the self-inductance of a loop is relatively small in our situation.

Examination of the loop inductance equations for only one turn shows them to be of the same general form regardless of the shape. If l [m] is the total perimeter of the figure and d [m] the diameter of the wire, then the inductance at high frequencies can be written ([18], Eq. (35)) as

$$L\,[\mathrm{H}] = \frac{\mu l}{2\pi}\left[\ln\frac{4l}{d} - \theta\right] \tag{4d}$$

The quantity θ is a constant that depends upon the shape of the loop. The value of θ for a circle is 2.451, for a square it is 2.853, and for a straight line $\theta = 0.75$. In the case of a square and $D \gg d$, Eq. (4d), which is of course identical to Eq. (4b), becomes

$$L_{\square}\,[\mathrm{H}] = \frac{2\mu D}{\pi}\left[\ln\frac{16D}{d} - 2.853\right] = \frac{8D}{10}\ln\frac{16D}{17.34d} \tag{4e}$$

and the expression for a circular loop ([18], Eq. (29)) is

$$L_{\bigcirc}\,[\mathrm{H}] = \frac{\mu D}{2}\left[\ln\frac{4\pi D}{d} - 2.451\right] = \frac{2\pi D}{10}\ln\frac{4\pi D}{11.6d} \tag{4f}$$

If the diameter of the winding is much bigger than the diameter of the wire, the ratio of the self-inductance of the square loop with respect to the circular loop is approximately

$$\frac{L_{\square}}{L_{\bigcirc}} \approx \frac{l_{\square}}{l_{\bigcirc}} = \frac{4}{\pi} \tag{4g}$$

Quite surprisingly, the ratio of the perimeters of the square and circular loops is identical to the ratio of their areas. Up to this point, already two ways have been found to optimize the self-inductance of a loop covering a given area in a telemetric system. The first possibility is decreasing the height of the loop as expressed with the help of Eq. (4c) and the other is increasing the perimeter of the loop, i.e., making it square (Eq. (4g)) or, even better, star or meander shaped. But there is a third interesting method: the number of turns can be increased by winding turns to the centre of a coil, which increases the self-inductance per unit area enormously. The geometrical parameters of a rectangular planar microcoil, which is not completely filled with turns, the wire having a diameter d [m], and having a pitch of winding $p = x_1 + b$ [m], are shown in Fig. 5. For such a coil the inductance is (see Eq. (4c) and [18], Eq. (48))

$$L_{\square}\,[\mathrm{H}] = \frac{2\mu s}{\pi}N^2\left[\ln\frac{s}{Np} + 0.2235\frac{Np}{s} + 0.726 - \frac{A+B}{N}\right]$$

$$= \frac{2\mu s}{\pi}N^2\left[\ln\frac{4s}{Np} + 0.894\frac{Np}{4s} - 0.660 - \frac{A+B}{N}\right] \tag{4h}$$

with A and B constants depending upon the wire spacing and number of turns, respectively. For $0.3p < b < 0.8p$, which is normally the case, the constant A is approximately $A = 2[(b/p) - 0.6]$. The constant B increases fast when the number of windings is still small but it saturates to $B \approx 0.336$ for higher N values ($N > 10$). In general, when $N > 10$ the influence of the factors A and B can be neglected. When we substitute $s = (D + D_i)/2$, $N = (D - D_i)/2p$, $\alpha = D_i/D$, and neglecting A and B, Eq. (4h) becomes

$$L_{\square}\,[\mathrm{H}] = \frac{\mu D^2}{4\pi p^2}(1-\alpha^2)(1-\alpha)$$

$$\times\left[\ln\frac{(1+\alpha)}{(1-\alpha)} + 0.2235\frac{(1-\alpha)}{(1+\alpha)} + 0.726\right] \tag{4i}$$

For a completly filled square coil $\alpha = 0$ and we arrive at

$$L_{\square}\,[\mathrm{H}] \sim 0.95\frac{\mu D^2}{4\pi p^2} \tag{4j}$$

3.2. Series resistance

The series resistance, R_S, of a coil can be divided into two parts; one is independent of and the other dependent on frequency. The frequency-independent part is the d.c. resistance of a wire, which is found by using Ohm's law. Consider a square coil in which the spiral does not completely extend to the centre (see Fig. 5). When we introduce the mean radius of the spiral as $a = (D + D_i)/4 = s/2 = (1+\alpha)D/4$, the total length is

$$l_{\square}\,[\mathrm{m}] = 8aN = \frac{D^2}{p}(1-\alpha^2) \tag{5}$$

and the total series resistance is then

$$R_{S\square}\,[\Omega] = \frac{\rho_{Cu} l}{hb} = \frac{\rho_{Cu} D^2}{h}\frac{1-\alpha^2}{bp} \tag{6a}$$

where ρ_{Cu} [Ω m] is the resistivity of the wire's material and h [m], b [m] and l [m] are the height, width and the total length of the wire, respectively. For a completely filled square coil $\alpha = 0$ and we arrive at

$$R_{S\,\mathrm{dc}}\,[\Omega] = \frac{\rho_{Cu} D^2}{bph} \tag{6b}$$

The frequency-dependent part of the series resistance is caused by strong time-varying magnetic fields produced by an alternating current which passes through the conductor. This field produces so-called eddy currents, which are local currents normal to the magnetic flux and opposite to the direction of the applied current. As the frequency increases, the current tends to shift to the surface of the wire, resulting in an uneven current redistribution in the inner wire leading to an increase in the series resistance. This phenomenon of current concentration on the outer 'skin' of the wire is known as the skin-effect. Moreover, the magnetic field causes eddy currents in adjacent wires and therefore also Ohmic power losses due to Joule heating. So, the high-frequency current is not only altering the local current distribution but also changes the current distribution in the rest of the coil. The skin depth δ [m] (or penetration depth), is given by [16]

$$\delta\,[\mathrm{m}] = \sqrt{\frac{2\rho}{\omega\mu}} \tag{7}$$

Only when the penetration depth is small compared to the diameter of the wire does this effect become important and the d.c. resistance has to be corrected due to redistribution of the current in the wire (see Appendix A). To give a rough estimation, when we incorporate the skin-effect into Eq. (6a) we get

$$R_{S\,\mathrm{ac}}\,[\Omega] = \rho_{Cu} D^2 \frac{1-\alpha^2}{p}\left(\frac{1}{hb} + \frac{1}{2\delta(h+b)}\right)$$
$$= \rho_{Cu} D^2 \frac{1-\alpha^2}{p}\left(\frac{1}{hb} + \sqrt{\frac{\omega\mu}{8\rho}}\frac{1}{h+b}\right) \tag{6c}$$

In our telemetric system, we are working with copper wires ($\mu_r \approx 0.999$ and $\rho \approx 2\times10^{-8}$ [Ω m]) typically 10 [μm] in diameter and at a frequency of 3 [MHz]. Therefore, the skin-depth equals $\delta \approx 0.07/\sqrt{f} \approx 40$ [μm], which is larger than the diameter of the wire so that the influence of the skin-effect on the total series resistance is negligible. Nevertheless, in telemetric systems working at high frequencies, the Ohmic 'd.c.' losses can be minimized by increasing the conducting area of the wire, but this profit is limited by the skin-effect. Moreover, increasing the width of a wire will decrease the maximum number of turns possible per unit area. So, a careful choice of the dimensions of the coil and working frequency of the circuitry is necessary.

3.3. Parallel resistance

The parallel resistance is caused by the finite resistance of the insulating layer on which the coil is placed. The power loss in this layer becomes influential at the moment when this resistance approaches the admittance of the capacitor, $X_C = 1/\omega C$. The parallel resistance is

$$R_{p\,\mathrm{ins}}\,[\Omega] = \frac{\rho_{ins} x_2}{bl} = \frac{\rho_{ins} x_2}{bD^2}\frac{p}{1-\alpha^2} \tag{8}$$

In most practical situations, the influence of the parallel resistance is far less than that of the series resistance. We will neglect it too.

3.4. Parasitic capacitance

The parasitic capacitance consists of three different capacities (Fig. 6(a)–(b)): the capacitance between the coil's turns C_{tt}, the capacitance between turns and substrate C_{st}, and the capacitance between contact pads and substrate C_{cs}. The electrical equivalent circuit is shown in Fig. 6(c). These capacitances might be approximated by those of parallel plates and, in the case of the unfilled circular coil and using Eq. (5), the expression becomes

$$C_{tt}\,[\mathrm{F}] = \frac{\epsilon h(l-4D)}{Nx_1} \approx \frac{2\epsilon hl}{x_1}\left(1+\alpha-\frac{4p}{D(1-\alpha)}\right) \tag{9a}$$

$$C_{st}\,[\mathrm{F}] = \frac{\epsilon bl}{x_2} \approx \frac{\epsilon bD^2}{x_2 p}(1-\alpha^2) \tag{9b}$$

$$C_{sc}\,[\mathrm{F}] = 2\frac{\epsilon A_{cp}}{x_2} \tag{9c}$$

where $\epsilon = \epsilon_0\epsilon_r = 8.84\times10^{-12}\epsilon_r$ [F m^{-1}] is the permittivity of the material between turns or between turn and substrate ($\epsilon_r = 1$ for air and $\epsilon_r = 3.8$ for SiO_2), x_1 and x_2 are the distances

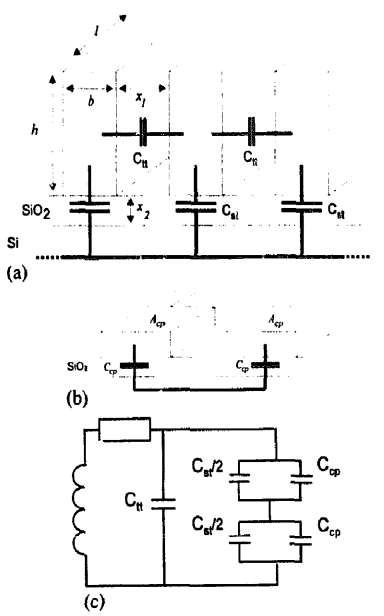

Fig. 6. Cross section of a planar coil showing the parasitic capacitances (a) between the turns C_{tt} and between turns and substrate C_{st}, (b) between contact pads and substrate C_{cp}; (c) electrical equivalent circuit of the parasitic capacitances.

between two adjacent turns and between turns and substrate respectively, and A_{cp} is the contact pad area. The factor N in the expression for C_{ss} is caused by the linearly decreasing voltage going from the outside of the spiral to its centre. The total parasitic capacitance C_{par} of the receiver coil is then given by

$$C_{par}\ [\mathrm{F}] = C_{ii} + \frac{1}{4}C_{si} + \frac{1}{2}C_{ss} \qquad (9d)$$

In our microcoil, the height of the wire h, and the distance between two adjacent turns x_1, are almost the same, but x_2 is much smaller. Therefore, it is allowed to neglect C_{ii}. Moreover, the contact pad is typically much smaller than the coil area, thus C_{ss} is negligible too, and we only have to consider C_{si}. So, in the case of a completely filled coil separated from a conducting substrate by only a relatively small distance, Eqs. (9b) and (9d) give

$$C_{si}\ [\mathrm{F}] = \frac{\epsilon b D^2}{4 x_2 p} \qquad (9e)$$

Sometimes, the parasitic capacitance caused by the conducting ground plane, such as the silicon wafer, is much too high. In such cases, the parasitic capacitance can be lowered drastically by replacing the oxidized silicon wafer by a glass substrate. Then, the capacitances to the substrate will be negligible with respect to the capacitance between the turns and only C_{ii} has to be calculated. Eq. (9a) is a simple parallel-plate approximation to estimate this capacitance. However, because the distance between the turns is typically of the same order as the diameter of the turns, Eq. (9a) cannot be used since electrical fringing, i.e., parasitic fields, start to play a role. A better estimation may be that of a capacitance between two long, parallel circular conducting wires of diameter d [13]:

$$C_{ii}\ [\mathrm{F}] = \frac{\pi\epsilon(l - 4D)}{N \ln\left(p/d + \sqrt{(p/d)^2 - 1}\right)} \qquad (9f)$$

where p is the pitch, i.e., the distance between the axes of two adjacent turns.

3.5. Quality-factor

The quality-factor or efficiency of the receiver coil of the telemetric system can now be calculated and optimized with respect to geometrical dimensions using the expressions just found (Eqs. (4i), (6a), (9b) and (9d)). After all, a coil with turns until the centre maximizes both the self-inductance and the series resistance. Since the self-inductance and the series resistance do not depend on the number of turns in the same way, there is a configuration which leads to an optimum ratio of self-inductance over resistance. This configuration is that of a coil with a small opening in the centre, i.e., the turns are not wound until the centre, which is expressed by way of the factor α. For an insulator with a negligible resistance R_s, this intrinsic Q-factor is (Eq. (1c))

$$Q_s = \frac{1}{R_s}\sqrt{\frac{L}{C_{par}}} = \frac{hbp}{\rho D^2(1-\alpha^2)} \times \sqrt{\frac{\mu D x_2 (1-\alpha)}{\pi\epsilon b p}\left[\ln\frac{(1+\alpha)}{(1-\alpha)} + 0.2235\frac{(1-\alpha)}{(1+\alpha)} + 0.726\right]} \qquad (10a)$$

This expression can be optimized with respect to the factor α, i.e., the ratio between the inner diameter and outer diameter of the planar microcoil. If we do so, we find that this maximum is reached for $\alpha = 1$, i.e., only one turn. This makes sense because the parasitic capacitance decreases linearly with the total length of the spiral until zero. Of course, $\alpha = 1$ is not a practical situation because it means that $D = D_i$ or there is no spiral at all.

As already mentioned, in our application we would like to tune both the receiver and transmitter units for the same frequency to couple energy as much as possible. Therefore, extra capacitors are placed in parallel with both coils. Such an extra tuning capacitor is possible as long as the intrinsic resonance frequency is lower than the desired operating frequency. Because we have settled the operating frequency of the receiving unit, the main parameter which determines the quality-factor in this case is the ratio between the reactance of the self-inductance and the series resistance as found by Eq. (1b):

$$Q_{ss} = \frac{\omega_s L}{R_s} = \frac{\mu\omega_s D h b (1-\alpha)}{4\rho p} \times \left[\ln\frac{(1+\alpha)}{(1-\alpha)} + 0.2235\frac{(1-\alpha)}{(1+\alpha)} + 0.726\right] \qquad (10b)$$

This ratio has its maximum at $\delta(L/R)/\delta\alpha = 0$, for $\alpha \sim 1/4$.

3.6. Mutual-inductance

The mutual-inductance M [H] between two coils (see Fig. 4) depends on the self-inductance of the transmitter coil L_1 and receiver coil L_2, and a parameter k which is a measure of the coupling and depends on the relative position of both the coils. When the relative position is such that lines of flux from one inductance link with turns of the other, the two inductances are said to be inductively coupled and mutual-inductance exists between them. Mutual-inductance may be defined in terms of the number of flux linkages in the second coil per unit current in the first coil, or vice versa. However, a more practical definition of the mutual-inductance is the voltage induced in the second circuit when the current in the first circuit is changing at a unit rate. If the current flowing in the first circuit is sinusoidal, then the voltage induced in the second circuit is

$$V_2 = M\frac{\mathrm{d}I_1(t)}{\mathrm{d}t} = M\frac{\mathrm{d}(I\sin\mathrm{j}\omega t)}{\mathrm{d}t} = \mathrm{j}\omega M I\cos\mathrm{j}\omega t \qquad (11)$$

Another quick method to find the mutual-inductance between two circuits is to measure first the self-inductance of a coil alone. Now, when a second coil is placed in the neighbourhood of this coil, the inductance of the first coil will change

by a value indentical to the mutual-inductance. The maximum value of mutual inductance that can exist between two coils is $\sqrt{(L_t L_r)}$, which occurs when all the flux of one coil is linked with all the turns of the other. The ratio of the mutual-inductance actually present to the maximum possible value that can occur is called the coefficient of coupling and is written as

$$k = \frac{M}{\sqrt{L_t L_r}} \tag{12a}$$

In general, the coefficient of coupling between two coils will only be close to one if the coils are quite close to each other. Close in this respect means that the distance between the two coils is smaller than their size. When both coils are tuned at the same resonance frequency, the coupling is at its maximum. For this so-called critical coupling k_c Eq. (12a) turns into

$$k_c = \frac{1}{\sqrt{Q_t Q_r}} \tag{12b}$$

When $k > k_c$, the resonance curve has two peaks and when $k < k_c$, the resonance curve is lower and smaller as in the case of $k = k_c$. In the case of two inductively coupled *LC*-circuits, Eq. (1b) should be modified. For such a 'band filter' the next expression holds:

$$Q_0 = \frac{\omega_0}{\omega\sqrt{2}}\sqrt{2} \tag{1d}$$

The factor $\sqrt{2}$ is caused by the extra *LC*-circuit with respect to Eq. (1b).

With the knowledge of the self- and mutual-inductances of the reciver and transmitter units, we are now able to calculate the energy transfer between both circuits. When the power in the transmitter circuit P_t is transferred by way of mutual-inductive coupling into the receiver unit, then the power received is

$$P_r\,[\mathrm{W}] = P_t\frac{M}{L_t} = \frac{1}{2}MI_t^2 \tag{13}$$

4. Design and fabrication of planar microcoils

In a telemetric system the major requirement is a high power transfer, so that as much power as possible is available for the implant. This means that the receiver coil should have a high Q, i.e., a high inductance value, a low series resistance and a low capacitance. An important problem with a microcoil is the decrease of the inductance due to the smaller area. This decrease can be compensated for by a large number of turns; however, the relatively long length of a spiral conductor required for a large number of turns produces a higher series resistance. For this reason it is desirable to use a low-resistivity coil material. In our case we decided to use copper, which has a resistivity of 2.0 μΩ cm (for thin films).

For an experimental evaluation we fabricated two types of coils, each 4.5 mm in diameter and 112 turns, which results in a pitch of 20 μm. The first planar coil (I) of 10 μm wire width, is 1 μm thick and lies on top of 1.9 μm of oxide. It is wound to the centre to maximize the self-inductance. The second coil (II) differs from the first in height of the conductor (11 μm), width of wire (14 μm), and thickness of the oxide layer (1 μm). All three have an influence on the quality of the coil at resonance, because an increase in conductor height and width decreases the series resistance and the decrease in insulator thickness increases the parasitic capacitance.

Two different fabrication techniques have been used to make the two types of coils: sputtering with lift-off (type I) and sputtering plus electroplating (type II). The main advantage of electroplating is the possibility of high structures. The fabrication of coil type II is schematically shown in Fig. 7. The process scheme was as follows: an adhesion layer of 20 nm Cr was sputtered on 1 μm silicon oxide, followed by 0.5 μm of Cu (step 1). Two layers of 7.5 μm thick resist (Ma-P275, Micro allresist) were spun on the wafer with a 1 min 90°C baking period in between (step 2). An electroplating set-up was made using a commercial Cu electrode and electrolyte (2.25 M H_2SO_4, 0.28 M $CuSO_4.5H_2O$ with surface-active agents). A layer of 11 μm of Cu was grown in 30 min (step 3) using the approximate formula for the growth rate δh at room temperature:

$$\delta h\,[\mu\mathrm{m\ min^{-1}}] = 0.016j \tag{14}$$

where a current density $j = 20$ mA cm^{-2} was used. After removal of the resist layer, the seed layer of sputtered Cr + Cu

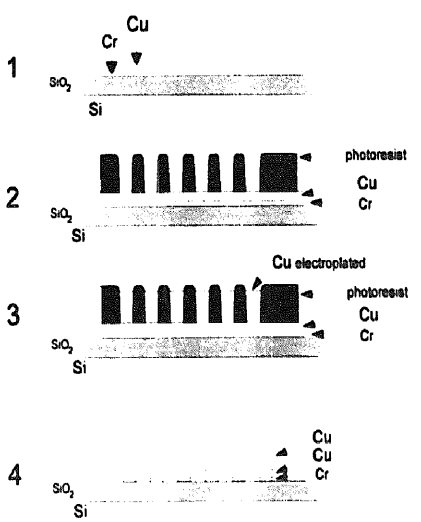

Fig. 7. Fabrication process for electroplated planar coil (II): step 1, after the deposition of the copper seed layer; step 2, spinning of the photoresist; this pattern can be used as a mould for step 3, the electroplating of a copper coil; step 4, the seed layer is locally removed by ion-beam etching.

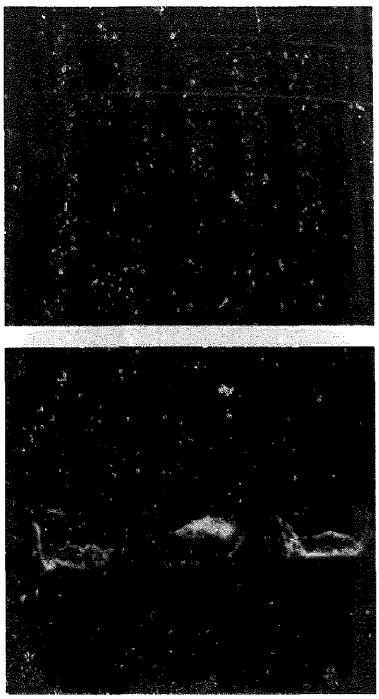

Fig. 8. SEM photographs of (a) top view of the centre, and (b) cross section of the electroplated coil (II).

Table 1
Parameters of the two coil configurations

Design parameter		Coil I	Coil II
D	outer diameter	4.50 mm	4.50 mm
D_i	inner diameter	0 mm	0 mm
α	ratio inner–outer diameter ($=D_i/D$)	0	0
N	number of turns	112	112
l	length of conductor ($=2ND$)	1.008 m	1.008 m
p	pitch between adjacent turns ($=D/2N$)	20 μm	20 μm
b	width of turns	10 μm	14 μm
h	height of turns	1 μm	11 μm
x_2	thickness oxide insulation	1.9 μm	1.0 μm
A_{cp}	contact pad area	1×0.5 mm^2	50×50 μm^2
Calculated parameters		**Coil I**	**Coil II**
L_s	self-inductance: Eq. (4j)	23.7 μH	21.6 μH
C_{tt}	capacitance between turns	0.008 pF	0.15 pF
C_{ts}	capacitance turns to substrate	179 pF	477 pF
C_{cs}	capacitance contact pads to substrate	17.5 pF	0.045 pF
C_{par}	total parasitic capacitance: Eq. (9e)	54 pF	119 pF
ρ	resistivity of thin-film Cu	2.0 μΩ cm	2.0 μΩ cm
R_{dc}	d.c. resistance: Eq. (6b)	2025 Ω	131.5 Ω
f_0	resonance frequency: Eq. (2a)		2.98 MHz
Q	quality-factor: Eq. (1c)		3.08
Z_0	characteristic impedance: Eq. (3c)		426 Ω
Measured parameters		**Coil I**	**Coil II**
R_{dc}	d.c. resistance	2060 Ω	129 Ω
f_0	resonance frequency		3 MHz
Q	quality-factor: Eq. (1d) and Fig. 12(b)		1.8
Z_0	characteristic impedance: Fig. 12(b)		405 Ω

was removed at unwanted locations by ion-beam etching (step 4). In Fig. 8, SEM photographs of the electroplated coil are shown. The surface of the electroplated copper is rough due to a quite high current density.

5. Results and discussion

The geometrical parameters of the coils and the calculated self-inductance (Eq. (4j)), d.c. resistance (6b) and parasitic capacitances (9e) are summarized in Table 1. Fig. 9 shows how the characteristics change with the filling of the coil, expressed with the variable $\alpha = D_i/D$. In all cases, the resistance and capacitance decrease when α increases. However, the self-inductance shows a maximum at $\alpha \approx 0.14$. The values at $\alpha = 0$ are the ones given in Table 1. Fig. 10 shows that the intrinsic resonance frequency and quality factor increase with α. When the frequency of the transmitter is settled to a constant value, let us say 3 MHz, the quality factor no longer increases with α. Instead it has a maximum at $\alpha = 1/4$ not depending on the real work frequency. Therefore, this factor is now called the operational or work quality factor. In general, the higher the intrinsic resonance frequency, the higher the frequency of the transmitter we can use and the better the performance with respect to the collected energy. Tuning of the receiver unit with an extra parallel capacitance will decrease the performance under all circumstances. The parasitic capacitance of the planar receiver coil is mainly determined by the capacitance between the turns and the substrate. Therefore, increasing the thickness of the insulating oxide will increase the intrinsic quality factor too. When a very high intrinsic quality factor is desired, then a glass substrate is useful.

The total impedance of the two configurations was calculated and the corresponding Bode diagrams are shown in Fig. 11. Coil I does not show a resonance peak. Instead, coil II exhibits a peak at 2.98 MHz, mainly due to the much lower series resistance.

Impedance measurements were performed using an HP 4194A impedance/gain phase analyser. The results are shown in Fig. 12. The 1 μm high coil does not show inductance, due to the relatively high series resistance of 2060 Ω (Fig. 12(a)). The electroplated coil II clearly shows inductance properties (Fig. 12(b)). The resonance frequency is 3 Mhz and the d.c. resistance is 129 Ω. The measured maximum impedance (405 Ω) is close to the theoretical value of 426 Ω, calculated for a d.c. resistance of 129 Ω. At 10 MHz there seems to be a second maximum in impedance. This might be caused by a difference in resonance frequency between the receiver and transmitter coil.

Table 2
Approximation of mutual-induction M and coupling factor k using coil II

Coil separation	M	k
1.0 mm	0.6 μH	0.036
3.5 mm	0.3 μH	0.018

The dependence of the energy transfer on the resistive load of the receiver circuit was measured using the transmitter–receiver set-up shown in Fig. 13(a). For first tests, a germanium diode (type AAZ15, $U_D = 0.3$ V) was used for single-sided rectification, in order to maximize the output voltage which drives the electronics. Of course, when the voltage is high enough, double-sided rectification is desirable to double the energy transfer to the load. Values of the several components are also displayed in this figure. The circuit was tuned to the resonance frequency of the sample coil. The output voltage and output power of the receiver coil V_r as a function of the load can be seen in Fig. 13(b),(c). Two different distances between the transmitter coil and the receiver coil, 1 mm and 3.5 mm, were used. The energy transfer can be as high as 2 mW. At a closer distance, the coupled flux is higher and, therefore, the voltage and power transfer is increased. The output voltage increases with the load resistance because the current through the load is decreasing. The power transfer to the load increases when the load decreases from 100 kΩ down to 400 Ω. The power transfer will be maximum when the load is adjusted to the characteristic impedance of the receiver LC-circuit, i.e., 426 Ω.

Using Eq. (11) and the measurements shown in Fig. 11, the mutual-inductance M and the coupling factor k can be approximated. These values are presented in Table 2. The values of the coupling factor seem quite low but are considered normal for this type of weak coupling.

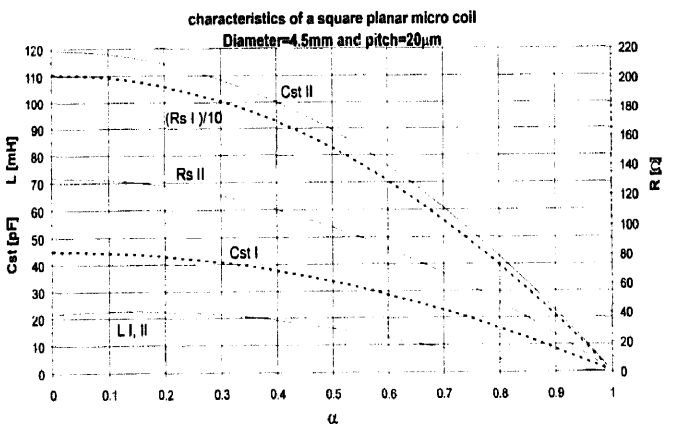

Fig. 9. Calculated Bode diagrams for two coil configurations considering parallel resistance to be negligible; width of the wire is 10 μm, height of coil (I) is 1 μm, and 10 μm for coil (II).

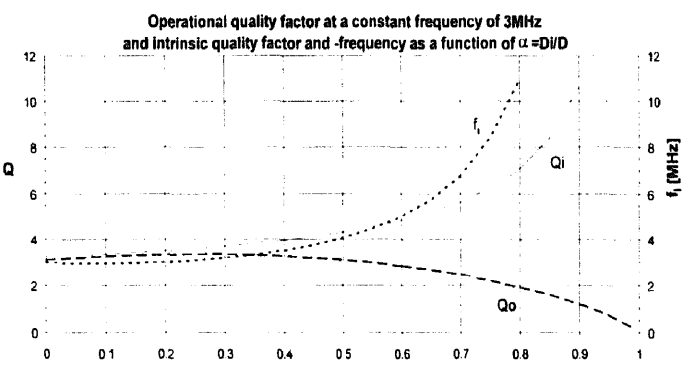

Fig. 10. Relationship between the operational quality factor at a constant frequency of 3 MHz and the intrinsic resonance frequency with its intrinsic quality-factor as a function of the ratio of the inner and outer diameters.

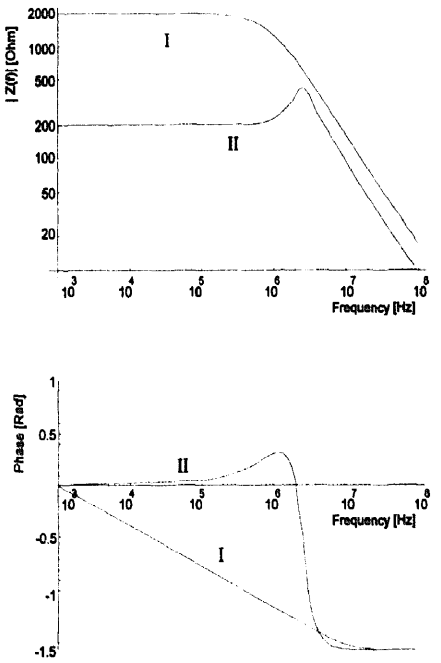

Fig. 11. Calculated Bode diagrams for two coil configurations considering parallel resistance to be negligible, width of wire is 10 μm for coil (I), 14 μm for coil (II), height of coil (I) is 1 μm, and of coil (II) is 11 μm.

6. Conclusions

This paper reports the fabrication, testing and characterization of an electroplated planar microcoil, which is used as the receiver coil in a telemetry system consisting of two inductively coupled coils. Calculations on the electrical parameters of the receiver coil have shown that for coils with a diameter of 4.5 mm and wire 14 μm in diameter, a few milliwatts can be transmitted. A gain in quality factor can be achieved (i) by making high structures, resulting in a decrease of the series resistance of the coil; (ii) by increasing the thickness of the insulator, or better, replacing the silicon substrate by a glass substrate; or (iii) by increasing the number of turns, since this increases the self-inductance enormously. When the frequency of the transmitter is fixed, then a little profit is gained by choosing a ratio between the inner and outer diameters of 0.25. When a glass substrate is used, the parasitic capacitance between the turns has to be taken into account. The described model for the electrical equivalent of the receiver coil predicts values of the intrinsic resonance frequency, intrinsic quality factor, series resistance of the coil and the power transfer from the coil into the load, which are in good agreement with measurements.

Acknowledgements

The authors would like to thank Erwin Berenschot, MESA Research Institute, for his technical assistance. This research project is supported by the Netherlands Technology Foundation (STW).

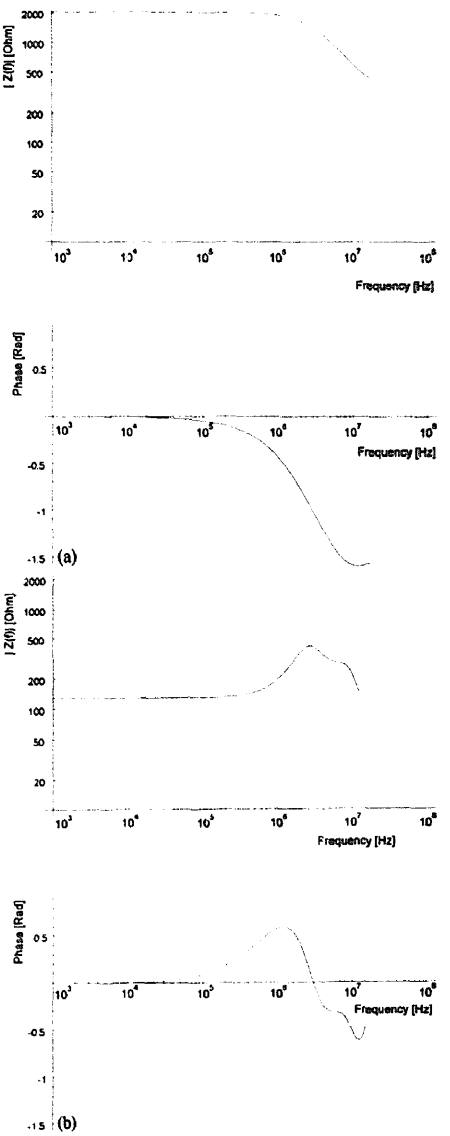

Fig. 12. Impedance measurements of (a) 1 μm high coil (I), and (b) 11 μm high coil (II).

Appendix A

At high frequencies, when the skin-effect becomes important, i.e., when the penetration depth, δ, is not negligible compared to the half-width of the wire, $b/2$, the resistance of a straight wire has to be corrected [8]:

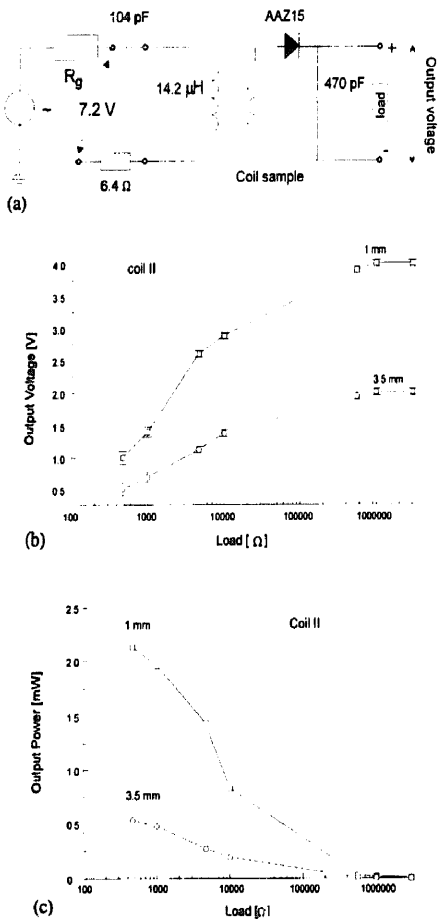

Fig. 13. (a) Transmission circuitry; (b) output voltage as a function of the load; (c) power dissipated by the load.

$$R_{\text{sac}}[\Omega] = R_{\text{d.c.}}\left[1+\frac{1}{48}\left(\frac{b/2}{\delta}\right)^4\right] \tag{18}$$

For two or more adjacent wires, the current distribution in one wire is affected by the magnetic field produced by the adjacent wire as well as by the magnetic flux produced by the current in the wire itself. This phenomenon, called the proximity effect, causes the resistance to be greater than in the case of the simple skin-effect. A formula which holds for a coil with only two turns is [11]

$$R_{\text{prox}} = R_{\text{d.c.}}\left\{1+\frac{1}{48}\left(\frac{b/2}{\delta}\right)^2\left[1+12\left[\left(\frac{b/2}{p}\right)^2 + \frac{1}{6}\left(\frac{b/2}{p}\right)^4 + \frac{1}{18}\left(\frac{b/2}{p}\right)^6 + \frac{1}{40}\left(\frac{b/2}{p}\right)^8 + \ldots\right]\right]\right\} \tag{19}$$

where p is the pitch, the distance between the axes of two adjacent turns. If $(b/2)/d \ll 1$, only the first term of the infinite series is relevant. For a single-layer disc coil with many spaced turns ($N > 35$), an approximate formula for the total resistance is [8]

$$R_{\text{total}}[\Omega] = R_{\text{d.c.}}\left\{1+\frac{1}{48}\left(\frac{b/2}{\delta}\right)^2\left[1+12u\left(\frac{b/2}{\delta}\right)^2\right]\right\} \tag{20}$$

The variable u depends on r_w/D (see Table 3), where D is the diameter and r_w is the winding depth of the coil. For a planar coil wound to the centre, the constant $u = 8.64$. The proximity losses can be neglected if $d > 2b$ [11].

An exact calculation of the frequency-dependent resistance is difficult to perform. For more accurate formulae, numerical methods are used [17].

Table 3
Correction parameter u for calculation of the effective resistance using Eq. (20). It depends on the winding depth r_w and diameter D of the coil. Values are from [8]

r_w/D	u	r_w/D	u
0.000	3.290	0.250	4.749
0.025	3.315	0.275	5.041
0.050	3.373	0.300	5.364
0.075	3.459	0.325	5.718
0.100	3.567	0.350	6.104
0.125	3.702	0.375	6.523
0.150	3.859	0.400	6.968
0.175	4.042	0.425	7.436
0.200	4.251	0.450	7.911
0.225	4.486	0.475	8.638
0.250	4.749	0.500	8.638

References

[1] R. Puers, Linking sensors with telemetry: impact on the system design, *Tech. Digest 8th Int. Conf. Solid-State Sensors and Actuators (Transducers '95/Eurosensors IX), Stockholm, Sweden, 25–29 June, 1995*, pp. 47–50.

[2] M. Nardin and K. Najafi, A multichannel neuromuscular microstimulator with bi-directional telemetry, *Tech. Digest, 8th Int. Conf. Solid-State Sensors and Actuators (Transducers '95/Eurosensors IX), Stockholm, Sweden, 25–29 June, 1995*, pp. 59–62.

[3] R. Kadefors, E. Kaiser and I. Petersen, Energizing implantable transmitters by means of coupled inductance coils, *IEEE Trans. Biomed. Eng., 16* (1969) 177–183.

[4] J.F. Lehmann, *Therapeutic Heat and Cold*, Williams and Wilkins, Baltimore, 3rd edn., 1982.

[5] J.R. Reitz, F.J. Milford and R.W. Christy, *Foundations of Electromagnetic Theory*, Addison-Wesley, Reading, MA, 1993.

[6] K. Kawabe, H. Koyoma and K. Shirae, Planar inductors, *IEEE Trans. Magn., MAG-20* (1984) 1804–1806.

[7] H.M. Greenhouse, Design of planar rectangular microelectronic inductors, *IEEE Trans. Parts, Hybrids, Packaging, PHP-10* (1974) 101–109.

[8] S. Butterworth, Effective Resistance of Inductance Coils at Radio Frequency: parts I and II. *Experimental Wireless and the Wireless Engineer*, (Apr.) (1926) 203–210 and 309–316.

[9] F.W. Grover, *Inductance Calculations: Working Formulas and Tables*, Dover, New York, 1973.

[10] J.M.C. Dukes, *Printed Circuits, their Design and Applications*, MacDonald, London, 1961, pp. 120–135.

[11] A.W. Lotfi and F.C. Lee, Proximity losses in short coils of circular cylindrical windings, *23rd Power Electrical Specialist Conf., IEEE PESC '92, Toledo, Spain, 29 June–3 July, 1992*, p. 1253–1260.
[12] H.A. Wheeler, Simple inductance formulas for radio coils, *Proc. IRE, 16* (1928) 1398–1400.
[13] E. Pettenpaul, H. Kapusta, A. Weisgerber, H. Mampe, J. Luginsland and I. Wolff, CAD models of lumped elements on GaAs up to 18 GHz, *IEEE Trans. Microwave Theory Tech., 36* (1988) 294–306.
[14] D. Lang, Broadband model predicts S-parameters of spiral inductors, *Microwaves and RF*, (Jan.) (1988) 107–110.
[15] D. Cahana, A new transmission line approach for designing spiral microstrips inductors for microwave integrated circuits, *IEEE MTT-S Int. Microwave Symp. Digest, Boston, MA, USA, 1983*, pp. 245–247.
[16] D.K. Cheng, *Field and Wave Electromagnetics*, Addison-Wesley, Reading, MA, 1989.
[17] P. Waldow and I. Wolff, Dual bounds variational formulation of skin effect problems, *IEEE MTT-S Int. Microwave Symp. Digest, Las Vegas, NV, USA, 1987*, pp. 333–336.
[18] F.E. Terman, *Radio Engineers Handbook*, McGraw-Hill, London, 1943, pp. 46–78.

Biographies

Cristina R. Neagu graduated from the University of Bucharest, Faculty of Physics, Romania, in 1990 with an M.Sc. degree in applied physics. From 1990 to 1993 she worked at the Institute of Atomic Physics, Bucharest. In 1993 she worked at the MESA Institute of the University of Twente, The Netherlands, on an investigation of human immunolabelled cells by atomic force microscope. Since 1994 she has been working for her Ph.D. at the Transducers and Materials Science Group at the same university, focusing on the design and realization of a pressure regulator based on micromachining techniques for biomedical application.

Henri V. Jansen received the M.Sc. (1991) degree in electrical engineering and the Ph.D. degree in physics (1996) from the University of Twente, The Netherlands. His research is concentrated on micro technology. Especially, the use of plasma chemistry is studied to sculpture micromachined structures. Currently, he is employed as a research assistant in the Department of Electrical Engineering at the University of Twente.

Ansgar Smith received the M.Sc. degree in electrical engineering from the University of Twente, The Netherlands, in 1996. He is currently employed as a technical support engineer for Access Graphics, Amstelveen, The Netherlands.

Johannes G.E. Gardeniers received the B.S. (1982) and M.S. (1985) degrees in chemistry and the Ph.D. degree in physics (1990) from the University of Nijmegen, The Netherlands. In 1990, he joined the Department of Electrical Engineering at the University of Twente, The Netherlands, as an assistant professor. His research interests include materials science and microfabrication technology related to microelectromechanical systems and miniaturized chemical analysis systems.

Miko Elwenspoek graduated from Freie Universität Berlin in 1977 on the physics of liquids. He received his Ph.D. in 1983 on nuclear quadrupolar relaxation in liquid alloys at the same university. From 1983 to 1987 he did research on crystal growth of organic materials from melt and solution at the University of Nijmegen, The Netherlands. Since 1987 he has been head of the Micromechanics Department at the University of Twente. Since 1 September 1996 he is professor of Transducers and Materials Science Group at the same university. He is a member of the MME (Micro Mechanics Europe) steering committee and of the MEMS steering committee. His research interests include: device physics, microactuators, microsensors, microsystems, etching mechanisms and technology.